Large etch-selectivity enhancement in the epitaxial liftoff of single-crystal LiNbO 3 films

A. M. Radojevic, M. Levy, R. M. Osgood Jr., A. Kumar, H. Bakhru, C. Tian, and C. Evans

Citation: Applied Physics Letters **74**, 3197 (1999); doi: 10.1063/1.124115
View online: http://dx.doi.org/10.1063/1.124115
View Table of Contents: http://scitation.aip.org/content/aip/journal/apl/74/21?ver=pdfcov
Published by the AIP Publishing

Large etch-selectivity enhancement in the epitaxial liftoff of single-crystal $LiNbO_3$ films

A. M. Radojevic,[a] M. Levy, and R. M. Osgood, Jr.
Microelectronics Sciences Laboratories, Columbia University, New York, New York 10027

A. Kumar and H. Bakhru
Department of Physics, State University of New York at Albany, Albany, New York 12222

C. Tian and C. Evans
Charles Evans and Associates, Redwood City, California 94063

(Received 14 January 1999; accepted for publication 25 March 1999)

We report on a large etch selectivity enhancement in the epitaxial liftoff of He^+-implanted single-crystal lithium niobate ($LiNbO_3$) films upon rapid thermal annealing. A buried sacrificial layer is formed by ion implantation. Heat treatment is found to reduce the time needed for film detachment by a factor as large as 100. Implant damage and postanneal stress-induced etch selectivity become nearly independent of implantation energy upon annealing. Large ($0.5 \times 1\ cm^2$) 5–10-μm-thick single-crystal $LiNbO_3$ films of excellent quality are detached in just a matter of a few hours. © *1999 American Institute of Physics.* [S0003-6951(99)02321-9]

Lithium niobate ($LiNbO_3$) is a technologically important ferroelectric material whose superior optical and dielectric single-crystal (SC) properties make it useful in a large variety of applications, ranging from optical fiber communications to wireless and micromechanical systems. The fabrication and integration of SC $LiNbO_3$ films of bulk-comparable properties onto heterogeneous planar substrates is therefore of significant technological importance.

The recent development of a novel epitaxial liftoff technique applicable to magnetic and ferroelectric oxides,[1,2] crystal ion slicing (CIS), has made it possible to obtain high-quality freestanding SC $LiNbO_3$ microns-thick films for integration into planar systems. Although a number of deposition techniques have been used in recent years to fabricate high-quality ferroelectric films on various substrates, many of the electrical and electro-optical figures of merit reported are generally not commensurate with those of the SC bulk.[3,4] Recent studies of several CIS film properties, however, show that the latter do retain or closely approximate SC features.[5] The CIS technique[1] employs the formation and subsequent preferential etching of a buried damage sacrificial layer obtained by implanting energetic He^+. Studies describing implantation-induced mechanical stress have been reported for metals and semiconductors.[6,7] Similar ion-implantation-based epitaxial liftoff techniques, albeit using very different separation mechanisms, have also been reported in high-dose, high-energy O-implanted diamond[8] and H^+-implanted Si.[9] As the ions penetrate into the target they scatter and lose energy. At higher energies along the trajectory, the scattering is primarily electronic and the process can be well described by the Linhard–Scharff–Schiott (LSS) theory.[10] Gradually, the ions become more susceptible to nuclear scattering. This process which, in turn, becomes a dominant stopping mechanism at lower ionic energies, is governed by Rutherford scattering (cross section $\sim 1/E^2$). The host nuclei thus become significantly dislodged towards the end of the ionic trajectories, leading to the formation of a narrow damage sacrificial layer well beneath the surface, which exhibits preferential etching upon immersion into 5% HF. Little residual damage is induced in the remainder of the film by the implantation.[1]

The scattering process described above assumes the absence of channeling, which would prevent the formation of a sharply localized implantation profile. Care has to be taken to minimize this effect and allow implant ions to deposit in a vertically very confined implanted damage layer.

In this letter we report on a large etch-selectivity enhancement in $LiNbO_3$ upon rapid thermal annealing (RTA), reducing the fabrication time and improving surface morphology. Upon implantation, He^+ does not go into solid solution in the host matrix; heat treatment thus drives the ions to regions of large damage where they coalesce, generating additional vertical stress. Our results show that He^+ pressure generated in the voids and the concomitant damage created in the sacrificial layer are not a strong function of implantation energy.

In this study, we focus on two different crystal geometries. A bulk $LiNbO_3$ crystal, *c* cut in one case and phase matched for second harmonic generation (SHG) at 1.55 μm in the other ($\theta=46.9°$, $\varphi=30°$), is cut from a *c*-poled single-crystal boule obtained by the Czochralski method. For the SHG films, the samples are sliced along the plane defined by the phase-matching direction and the o-ray polarization direction at 1.55 μm. The samples are implanted with He^+ ($5\times10^{16}\ cm^{-2}$ dosage) at a tilt angle of 3° relative to the sample normal. Several ionic energies ranging from 3.18 to 3.8 MeV, which correspond to penetration depths of 8–10 μm, respectively, based on TRIM96 calculations, are used in order to probe the effect of film thickness on etching and SHG.[11] Irrespective of the initial ion energy, the straggle in the projected ion range remains almost unchanged. The implanted samples are rapid thermal anneal (RTA) treated in forming gas (5% H_2, 95% N_2) under various conditions and

[a]Electronic mail: tony@cumsl.ctr.columbia.edu

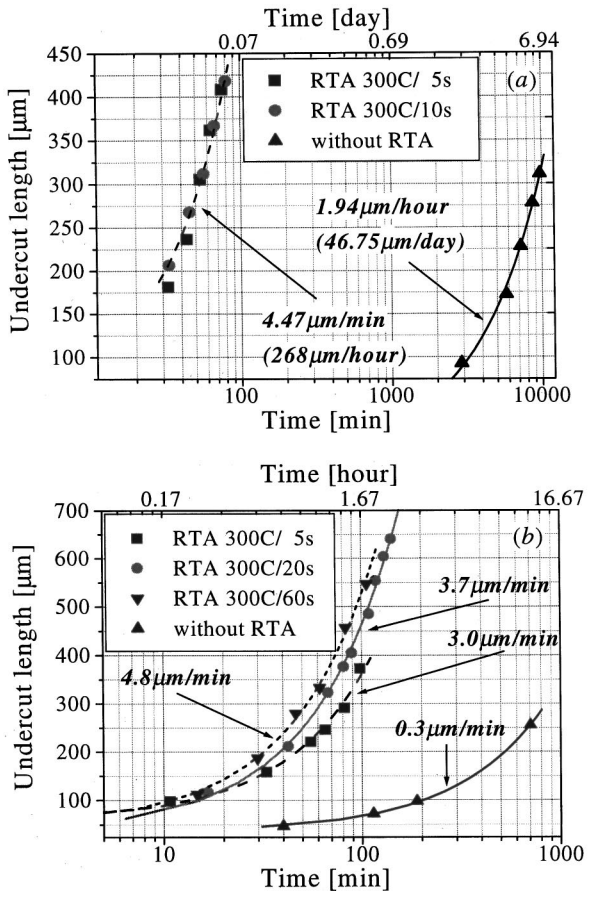

FIG. 1. The effect of RTA on undercut time evolution in SHG $LiNbO_3$ implanted with (a) 3.18 MeV He^+ (the etch-rate enhancement factor >140) and (b) 3.8 MeV He^+ (the etch-rate enhancement factor >15).

then etched. A deep undercut forms in the sacrificial layer and uniformly (its front parallel to the facets) progresses with time, resulting in a freestanding CIS film. The undercut length is easily determined using Nomarski prism optical microscopy, by measuring the extent of the interference pattern created by the air gap between the partially lifted-off film and the substrate.

Different annealing temperatures (250–700 °C) and times (5–60 s) were studied: 300 °C was found to be the optimum for the SHG films, while for the *c*-cut geometry 400 °C yielded significant etch-rate enhancement. While the unannealed SHG control samples have slow etch rates (~50 μm/day/facet for 3.18 MeV, and ~20 μm/h/facet for 3.8 MeV implants), the annealed samples exhibit a uniform undercut formation after only ~2 min in the etchant. In comparison to the control sample, an etch-rate enhancement of more than 140 is obtained for the annealed 3.18 MeV implants [Fig. 1(a)]. This high etch rate permits CIS films of excellent surface quality and as large as 20–50 mm^2 to be detached in just a matter of a few hours. In all cases the undercut length is a linear function of time, contrary to the standard epitaxial liftoff in III–V materials where etch saturation is observed.[12] The etch-rate enhancement for higher implantation energies [Fig. 1(b)] is greater than 15, but these samples already have higher etch selectivities before annealing. In fact, after-anneal etch rates are very close for all implantation energies, although the preannealed sample rates differ markedly (Table I). The results also show that longer RTA exposures yield higher etch rates.

TABLE I. Etch rates before and after RTA for different crystal geometries/ion energies.

Sample	Rates before RTA	Rates after RTA
3.18 MeV SHG	~2 μm/h	~4.5 μm/min[a]
3.5 MeV SHG	not recorded	~5 μm/min[b]
3.8 MeV SHG	~20 μm/h	~5 μm/min[b]
3.8 MeV *c* cut	~20 μm/h	~3 μm/min[c]

[a]RTA 300 °C/30 s.
[b]RTA 300 °C/60 s;
[c]RTA 400 °C/30 s.

Figure 2 shows a scanning electron micrograph of a freestanding $LiNbO_3$ CIS film for SHG with its underside facing up. although the top surface remains smooth, the underside is decorated with shallow parallel grooves, 0.1 μm deep, that follow the phase-matching direction. These grooves are crystal-orientation dependent and stem from the interaction of the implantation charge with the ferroelectric polarization during the implant and etching process. This phenomenon, which will be reported elsewhere, has been found to have no implications for the dielectric and optical properties of the freestanding films.

For *c*-cut $LiNbO_3$ only one implantation energy (3.8 MeV) was studied. In this case, initial etch rates of ~20 μm/h/facet increase to ~180 μm/h/facet for the RTA pretreatment at 400 °C for 30 s, increasing the etch rate by a factor of ~9. As a result, a complete CIS film processing for a 2 mm × 10 mm sample requires ~6 h, which is ~1.5× the etch time of the annealed SHG samples. Thus the post RTA treatment etch rates are nearly geometry- and implantation-energy independent. The shallow grooves observed on the underside of the SHG films are also seen in the *c*-cut films and are of comparable depth. The difference, however, lies in the structure and orientation of the lines, as in the latter case the grooves form a trigonal pattern.[1] Interestingly, this trigonal structure disappears upon annealing, resulting in a uniform undercut evolution, and thus a smooth film surface.

To study the effect of annealing on ion distribution, secondary ion mass spectroscopy (SIMS) was performed on both crystalline geometries. The composition profiles were analyzed using Cs^+ as the primary directed ion and MCs^+ as the secondary detected species. Here M refers to Li, Nb, and

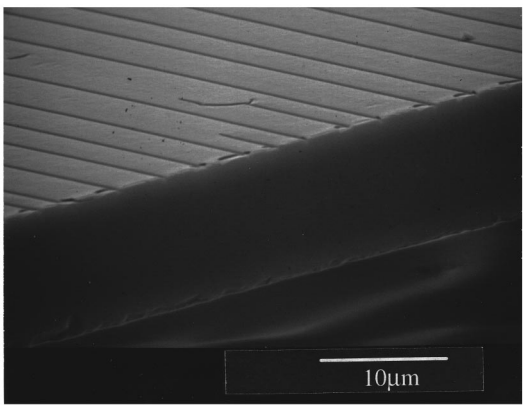

FIG. 2. An electron micrograph of a CIS $LiNbO_3$ film oriented for SHG (3.8 MeV He^+ implantation, RTA at 300 °C/60 s). The underside grooves follow the phase-matched direction.

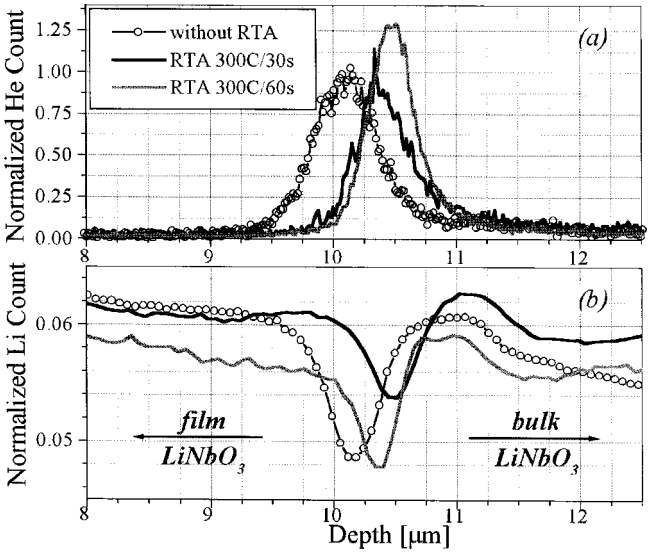

FIG. 3. SIMS (a) He^+ and (b) Li area-normalized spectra before and after RTA in 3.8 MeV He^+-implanted $LiNbO_3$ for SHG. No He^+ loss is assumed during RTA. The offset in Li spectra is a measurement artifact.

O. The choice of MCs^+ stemmed from the smaller sensitivity of the ion yield to the crystal matrix.[13] Helium profiling was performed with O_2^+ as the primary ion and required additional surface charge compensation, which was accomplished by electron flooding of the sputtered area.

Figure 3 depicts the change in He^+ and Li spectra upon RTA in implanted samples for SHG (*c*-cut implants have similar spectra). The observed ion range is in good agreement with the TRIM96 predicted value, consistent with the absence of significant channeling.

The study shows that the postanneal He^+ distribution evolves towards sharper and narrower spectra, thus yielding an increase of the internal pressure in the sacrificial layer. Due to its low solid solubility, He^+ tends to fill in the implantation-generated microvoids. The high Li mobility allows it to be displaced and replaced by He^+. The peak in the He^+ spectrum is shifted deeper into the bulk with increasing annealing exposure, while a depletion dip in Li spectra follows the same trend [Fig. 3(b)]. This thermal evolution of internal voids and corresponding pressure buildup in the sacrificial layer are responsible for the enhanced etch selectivity observed in thermally treated samples. A similar phenomenon, albeit with an entirely different chemistry and diffusion characteristics, has been reported for H^+ and He^+ coimplantation in Si.[14]

Tests conducted at higher anneal temperatures ($>500\,°C$) do, in fact, lead to exfoliation in the implanted samples, corroborating the presence of a large internal pressure buildup in the sacrificial layer. Although film stripes of relatively large area ($\sim 1\ \text{mm} \times 5\ \text{mm}$) can be recovered, the process itself is not controllable and in most cases results in destructive sample delamination. Interestingly, the observed exfoliation does not require the affixing of a wafer stiffener to the implanted surface, as in the case of the Smart-Cut delamination in Si.[9]

The implantation-energy independence in the etch selectivity of the heat-treated samples can also be related to the evolution of microvoids and internal pressure. Thus, the postanneal stress in the material and broken interatomic bond distribution results in comparable etch rates, regardless of the implantation energy in the bias range studied here.

In conclusion, we have presented a technique for rapid micron-thick $LiNbO_3$ SC film processing. Different $LiNbO_3$ crystal geometries exhibit similar etch behavior upon annealing. High-quality SC thin films of sizes commensurate with the standard $LiNbO_3$ device dimensions and of unchanged bulk stoichiometry can be fabricated in a short period.

This work was supported in part by AFOSR/DARPA program (Contract No. F49620-99-1-0038) and in part by DARPA FAME program (Contract No. N0017398-1-G014). The authors gratefully acknowledge helpful discussions with L. E. Cross, A. Bhalla, and R. Liu.

[1] M. Levy, R. M. Osgood, Jr., R. Liu, L. E. Cross, G. S. Cargill III, A. Kumar, and H. Bakhru, Appl. Phys. Lett. **73**, 2293 (1998).
[2] M. Levy, R. M. Osgood, Jr., A. Kumar, and H. Bakhru, Appl. Phys. Lett. **71**, 2617 (1997).
[3] G. Griffel, S. Ruschin, and N. Croitoru, Appl. Phys. Lett. **54**, 1385 (1989).
[4] T. A. Rost, H. Lin, T. A. Rabson, R. C. Baumann, and D. L. Callahan, J. Appl. Phys. **72**, 4336 (1992).
[5] R. Liu, R. Guo, A. S. Bhalla, L. E. Cross, M. Levy, and R. M. Osgood, Jr. (unpublished).
[6] N. Hartley, J. Vac. Sci. Technol. **12**, 485 (1975).
[7] J. S. Williams, Phys. Lett. A **60A**, 330 (1977).
[8] N. R. Parikh, J. D. Hunn, E. McGucken, M. L. Swanson, C. W. White, R. A. Rudder, D. P. Malta, J. B. Posthill, and R. J. Markunas, Appl. Phys. Lett. **61**, 3124 (1992).
[9] M. Bruel, Electron. Lett. **31**, 1201 (1995).
[10] J. Lindhard, M. Scharff, and H. E. Schiott, Mat. Fys. Medd. K. Dan. Vidensk. Selsk. **33**, 14 (1963).
[11] A. M. Radojevic, M. Levy, and R. M. Osgood, Jr. (unpublished).
[12] E. Yablonovitch, T. Gmitter, J. P. Harbison, and R. Bhat, Appl. Phys. Lett. **51**, 2222 (1987).
[13] Y. Gao, J. Appl. Phys. **64**, 3760 (1988).
[14] M. K. Weldon, M. Collot, Y. J. Chabal, V. C. Venezia, A. Agarwal, T. E. Haynes, D. J. Eaglesham, S. B. Christman, and E. E. Chaban, Appl. Phys. Lett. **73**, 3721 (1998).